All reflective THz telescope design with an inflatable primary antenna for Orbiting Astronomical Satellite for Investigating Stellar Systems (OASIS) mission

Yuzuru Takashima[a*], Siddhartha Sirsi[a,c], Heejoo Choi[a,b], Art Palisoc[d], Jonathan W. Arenberg[e], Daewook Kim[a,b,c] ,Christopher Walker[a,c],

[a]Wyant College of Optical Sciences, University of Arizona, 1630 E. University Blvd., Tucson, AZ 85721, USA
[b]Large Binocular Telescope Observatory, University of Arizona 933 N Cherry Avenue, Tucson, AZ 85721, USA
[c]Department of Astronomy and Steward Observatory, University of Arizona, 933 N. Cherry Ave., Tucson, AZ 85721, USA
[d]L'Garde, Inc., 15181 Woodlawn Avenue, Tustin, CA 92780, USA
[e]Northrop Grumman Aerospace Systems, 1 Space Park Blvd, Redondo Beach, CA 90278

ABSTRACT

With an inflatable membrane, a space antenna having an order of magnitude larger photon collection area as compared to the state of the art is feasible. An integrated and comprehensive study has been performed by the scientists and engineers team at NASA Goddard, Northrup Grumman, L'Garde and University of Arizona. As a part of the study, optical design for the 19m antenna is overviewed here.
K**eywords:** Teraheltz astronomy, space antenna, inflatable primary mirror, Hencky surface

1. INTRODUCTION

The Orbiting Astronomical Satellite for Investigating Stellar Systems (OASIS) is a 17 meter class space observatory concept that will perform heterodyne and high spectral resolution observations at terahertz wavelength ranging from 81 to 659 micrometers to observe the transition of water and its isotopologues and other molecular species[1]. The baseline design, in particular with an inflatable primary antenna achieves orders of magnitude larger photon collection area, > 120 m^2 and diffraction limited performance at field of view (FOV) of +/- 0.05 deg with a simple tip/tilt scanner and over 0.2 degrees with an advanced scanning field lens design. The THz observatory with such an inflatable primary system involves an interesting challenge in optical design. The surface shape of the inflatable primary antenna, known as Hencky surface, induces 4th or higher order deformation of reflector surface which is corrected by following 3-mirror correction optics, with a power arrangement which is similar to Offner's null corrector optics. The same optical architecture is also applicable for more parabola like inflatable antenna shape. The diffraction limited intermediate image field is scanned by a mirror tip-tilt scanner, alternatively for a larger FOV scanning a field lens, refractive or reflective, rigidly connected to the scanning mirror is employed. The design with thin reflective field lens or all refractive design increases overall photon throughput while accommodating broad band spectral range. Along with the 1st and 3rd order optical design procedure, in this presentation, We address challenges in optical design of such a large and inflatable antenna based photon collection system in THz astronomy, including correction of aberration from a membrane antenna, and relay optics to match mode field of antenna to that of THz heterodyne detectors.

2. OPTICAL DESIGN FOR OASIS

2.1 Optical architecture

Figure 1 illustrates the concept of the OASIS observatory. The 17m primary antennal A1 is initially stored during launching and deployed once space craft is in place [2]. The deployment process involves inflation of the A1 antenna as well as three

Astronomical Optics: Design, Manufacture, and Test of Space and Ground Systems III, edited by Tony B. Hull, Daewook Kim, Pascal Hallibert, Fanny Keller, Proc. of SPIE Vol. 11820, 118200P · © The Authors. Published under a Creative Commons Attribution CC-BY 3.0 License doi: 10.1117/12.2594610

booms that supports the A1 antenna. For the purpose of inflation, the A1 antenna is made of two membranes, front canopy and back reflector surfaces [3]. The front canopy is a 0.5 mil black Kapton to block visible to infrared sunlight and is transparent for the wavelength range for observation. The 2nd surface of the antenna is aluminum coated thin film membrane that collects photons from science targets [1]. The space in between two membranes is pressurized to form a concave reflective surface. The wavelength of OASIS mission ranges from 81um to 656um. The telescope has to be highly efficient over the wavelength range to accommodate large geometrical photon collection area of >110 m2 at the shortest wavelength while keeping a diffraction limited photon delivery of F/16 beam matched to the heterodyne detector system [1].

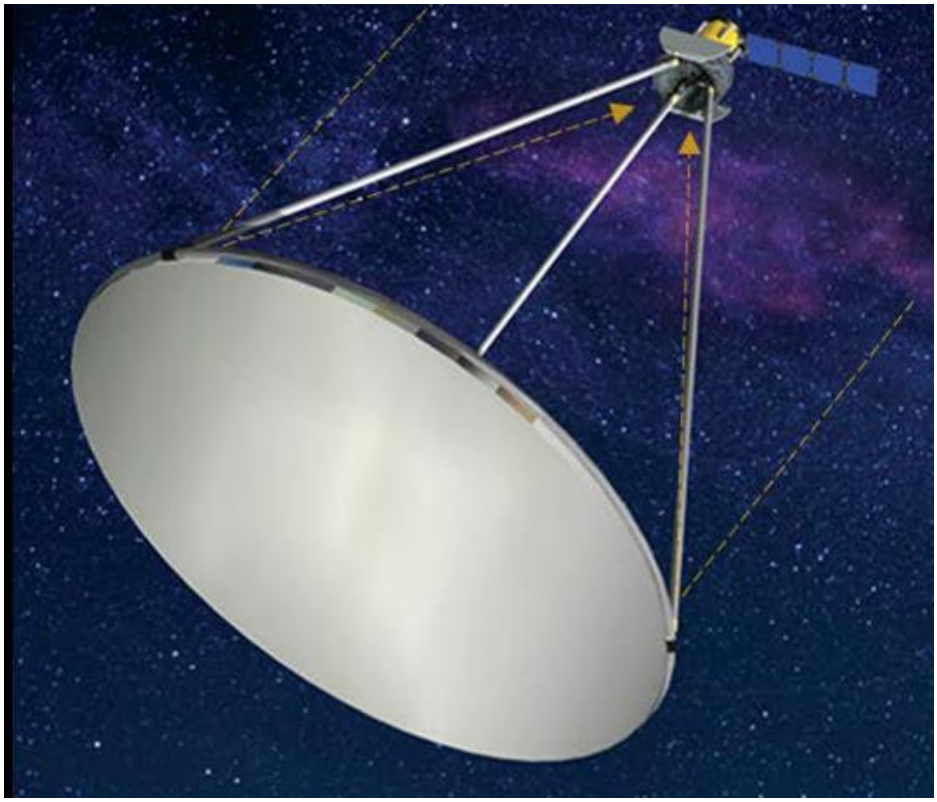

Fig. 1 OASIS observatory in space. With 17m inflatable primary antenna, over 100m^2 effective photon correction area is supported.

Due to the inflatable nature of the primary antenna A1, the surface figure of antenna deviates from a parabolic shape. One of the well-studied shapes of such inflatable antenna is a Hencky surface [4]. The Hencky surface is a shape of circular membrane when that surface is uniformly pressurized while the edge of the membrane is rigidly constrained. Another example of such membrane based inflatable antenna is using a pre-cut-gore that are glued together and pressurized to inflate it [5]. The pre-cut gore is a pizza slice like flat membrane. The shape of the pre-cut gore is determined to form a quasi-parabola after being inflated. As expected, the inflated shapes of A1 has a substantial deviation from the ideal parabolic shape, several tens of waves, even with the pre-cut-gore time membrane.

To correct for the deviation of A1 surface from ideal parabola, a reflective corrector optics M2 and M3 are incorporated as depicted in the inset of Fig. 2. The M2 M3 mirror pair simultaneously compensates for the deviation of A1 from parabola shape as well as off axis aberrations such as Coma.

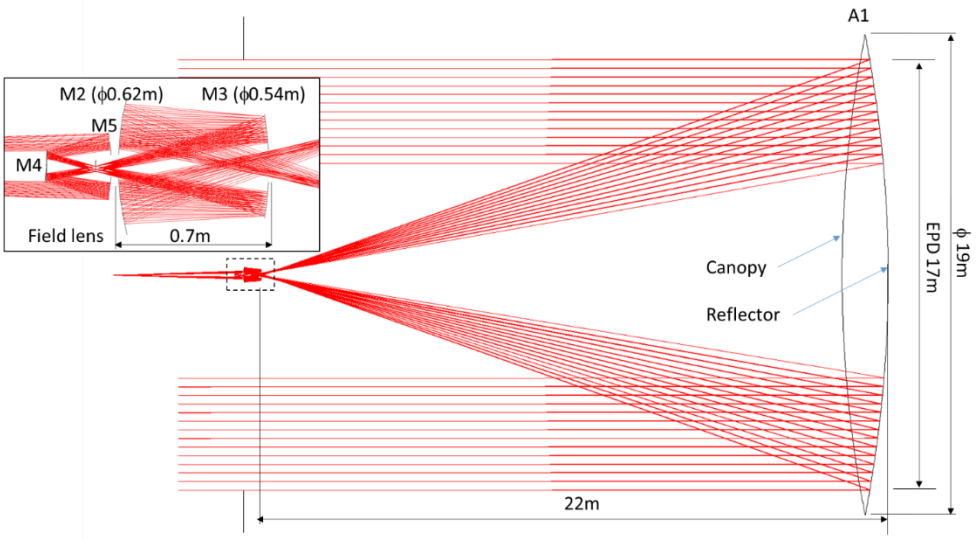

Fig. 2. Optical layout of OASIS antenna system. The inset shows correction optics M2, M3 and FOV scanner M4 and M5.

Table 1 summarizes primary design parameters of OASIS telescope.

Table 1. OASIS design parameters.

Specification items	Design results
Entrance pupil diameter	17 m
A1 focal length	25 m
System F/#: $(F/\#)_{system}$	16
Field of View [degrees]	+/- 0.05 degrees
Wavelength	658.88 to 521.38 μm
	272.54 to 136.27 μm
	121.13 to 104.28 μm
	81.42 to 81.2 μm

2.2 Impact of A1 aberration on corrector optics design

Among challenges of the optical architecture employing an inflatable A1 antenna, uncertainity of the inflated shape of A1 is one of the critical ones that defines fabrication process of M2 and M3. The control of the inflated shape in orbit is also a challenge especially under variation of altitude of sun during the mission. The non-uniform temperature distribution over the surface deforms the A1 antenna surface that deteriorates photon collection efficiency due to the decrease in coupling efficiency of aberrated beam to detector. The fabrication process is describes elsewhere [2]. The process involves metrology of the surface followed by design of M2, M3 based on the measurement. The M2, M3 is diamond turned surface. Thanks to the longer wavelength > 81um, the surface accuracy of M2 and M3 is considerably low as compared to those corrector optics in visible to near infrared telescopes. For quick turnaround of such measure and fabricate process, optical design of corrector optics especially its size needs consideration. Smaller, compact, and light weight optics considerably reduces the fabrication lead time and launch cost.

Two approaches in fabricating A1, Hencky reflector, and pre-cut-gore reflector are compared in optical design. Figure 3 compares optical layout of A1-M2-M3 for a) Hencky and b) preformed gore inflatable A1. One may observe that there is

a substantial difference in the diameter of M2 and M3 as well as spacing between M2 and M3. The difference in the dimensions, sizes and spacing between the two A1 designs are understood from the functionality of M2 and M3. The M2 is placed at paraxial focus of A1 and functions as a filed lens that corrects for spherical aberration of A1. M3 is relaying the paraxial focus again at M2 with 1:1 imaging ratio. In this manner M3 works as a relay with unit magnification. A relay lens placed at paraxial focus of primary parabolic is previously known in a literature to correct for spherical aberration [6]. The diameter of M2 is basically blur size of A1 at the paraxial focus, and is an extent of the transverse ray aberration ε_y that is given by,

$$\varepsilon_y = -2(F\#)\frac{\partial W}{\partial y} \quad (1)$$

$$W = w_{040}y^4 + w_{060}y^6 + \cdots \quad (2)$$

Where y is a pupil coordinate normalized by half diameter of pupil size, and the terms $w_{040}, w_{060}, ..$ are 4th and 6th order terms of wave aberration and so on. F/# is f-number of A1 antenna. For example, it is known that the extent of the ε_y at the presence of w_{040} is $16(F/\#)w_{040}$. In this manner, the M2 diameter simply depends 4th or higher order spherical aberrations terms. Due to the 1:1 relay configuration, the M2-M3 distance linearly scales with focal length of M3. With a larger aberration terms, a longer M2-M3 spacing d_{2-3} is required to correct A1 induced aberrations by increasing F/# of M3 and decreasing chief ray angle impinging on M3. Consequently, the M3 diameter scales with $d_{2-3}/(F/\#)_{System}$ since A1-M2-M3 system $(F/\#)_{System}$ is approximately same as F/# of A1, $(F/\#)_{A1}$ [7]. The corrector optics M2 and M3 are substantially compact once a pre-cut-gore based A1is employed as compared to the M2 M3 optics for Hencky A1 antenna.

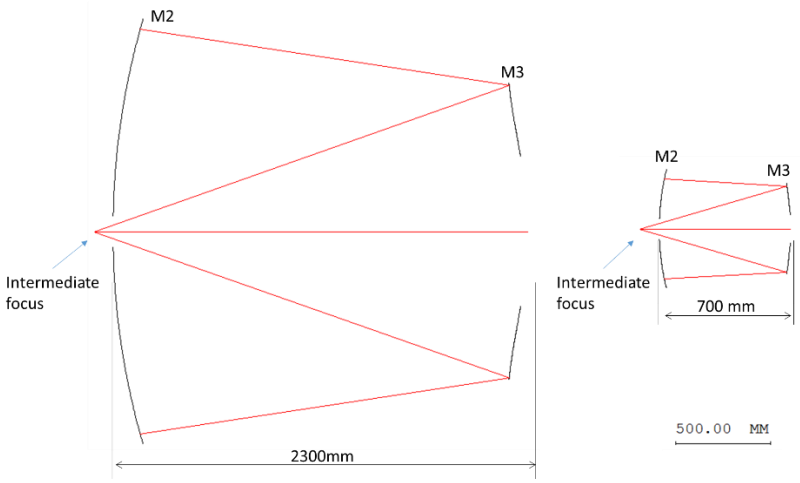

a) b)

Fig. 3. Optical layout of OASIS corrector for a) Hencky A1 and b) pre-cut-gore A1 having the same base radius of curvature R1 = 50m, plotted is the same scale.

For Hencky primary mirror, the aspheric terms A2 and A4 are analytically identified for R1. For the quasi parabolic A1, inflated shape of calculated by proprietary code FAIM-FLATE [5] for three values of R1 = 40, 50 and 60m. We found that decreasing pressure about 20% from the nominal pressure provides the closest shape to the parabola. The decreased pressure value was adopted for the analysis. The smaller diameter of correction optics M2 and M3 and shorter spacing between them is an obvious advantage of using pre-cut gore based A1. Also pressure requirement is about 1/7 for the pre-cut gore based A1 that substantially decreases the amount of gas by 1/7 accordingly that balances launch mass and duration of mission [5].

2.3 FOV scanner design

OASIS supports the field of view (FOV) of +/- 0.05 [deg] by scanning the intermediate image (in Fig. 3) with a tip tilt mirror. Figure 4 depicts the layout of the FOV scanner optics. The intermediate image is first scanned by a tip-tilt mirror, then it is re-imaged to the detector module via ellipsoidal mirror. In the OASIS optical design, the stop is placed at A1. The M2 relays the entrance pupil, which is A1 itself, to approximately to the location of the M3. To minimize the size of scanning mirror while avoiding a vignetting during the scanning, field lens is placed at the intermediate focal plane. For the design supporting FOV of +/- 0.03 degrees, a high resistivity Si lens with central thickness of 2mm, and diameter of 60mm is placed to relay the exit pupil of A1-M2-M3 telescope (M3) to scanning tip/tilt mirror (M4). The absorption loss of refractive lens is of concern, however the 2mm thick of the lens has a negligible effect on overall photon collection efficiency [8]. The high resistivity lens also blocks sun light along with by the black Kapton as front shield that protects the detector assembly from being damaged or malfunctioning by strong stray light.

Current OASIS scanner employs a single refractive field lens. Upon requirement for even a larger FOV of +/- 0.1 [deg] or more, moving and reflective field lens architecture is an option to minimize absorption loss (Fig. 5). A reflective field lens pair (a pair of aspheric concave mirrors) is rigidly connected to M4 that scans the FOV. This scanning field lens design scans a larger intermediate field as compared to the static field lens design. The reflective and moving field lens design supports even wider FOV of +/- 0.1 degrees.

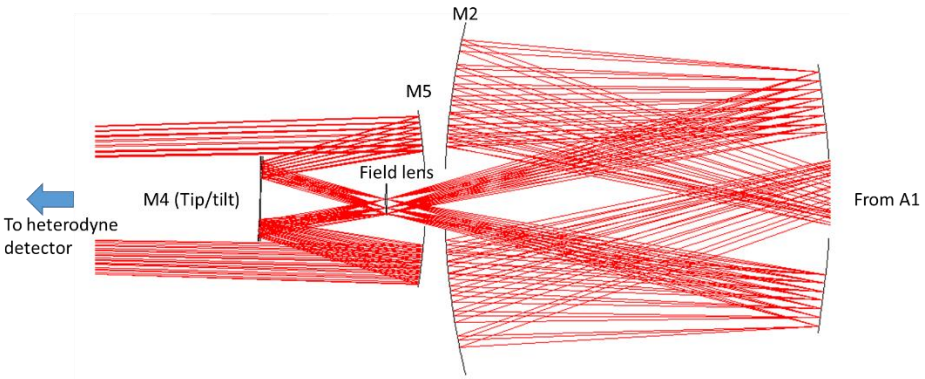

Fig. 4. Optical layout of OASIS scanner for pre-cut-gore A1 having base radius of curvature R1 = 50m. At the intermediate image place behind the M3, a high resistivity Si filed lens is placed to map the exit pupil of A1-M2-M3 to tip/tilt mirror M4. In the figure ray path corresponding to the FOVs, 0, 0.03 and 0.05 degrees are overlaid.

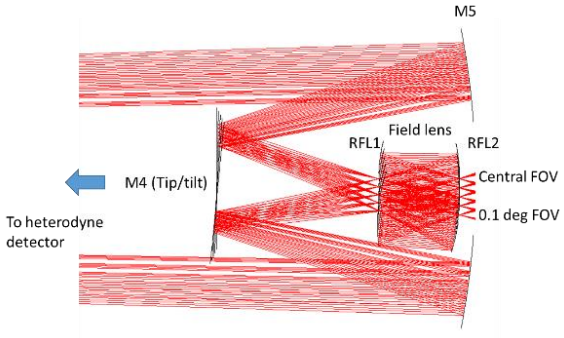

Fig. 5. Optical layout of OASIS scanner. At the intermediate image place behind the M3, a pair of reflector (RFL1 and RFL2) are placed to map the exit pupil of A1-M2-M3 to tip/tilt mirror M4. The RFL1 and RFL2 mirrors are rigidly connected to M4. In the figure ray path corresponding to the FOVs, 0, 0.025, 0.05, 0.075 and 0.1 degrees are overlaid.

Table 2 tabulates as design performance of antenna and corrector optics (A1-M2-M3) and total system including the scanner. The system is designed so that the A1-M2-M3 and scanner is individually evaluated in optical performance,

followed by integrating them. At the shortest science wavelength of λ = 81um, the as deign performance of about λ/10 RMS. At the longer wavelength, the as design performance is diffraction limited ones.

Table 2. Wave aberration in RMS for A1-M2-M3 antenna and as a total system.

	Wave aberration in RMS [um]
A1-M2-M3, On-axis/Off-axis	4.28/7.65
Total system, On-axis/Off-axis	5.61/4.17

Figure 6 depicts optical layout of OASIS corrector, scanner and folding optics. An intermediate image formed on a field lens by A1-M2-M3 optics. M4 (tip/tilt mirror) and M5 relays the intermediate image to single point where detector input port is placed. Folding optics FM1, 2, 3, 4 and 5 folds optical path. Dimensions of each of optical components are tabulated in Table 3 along with its loss.

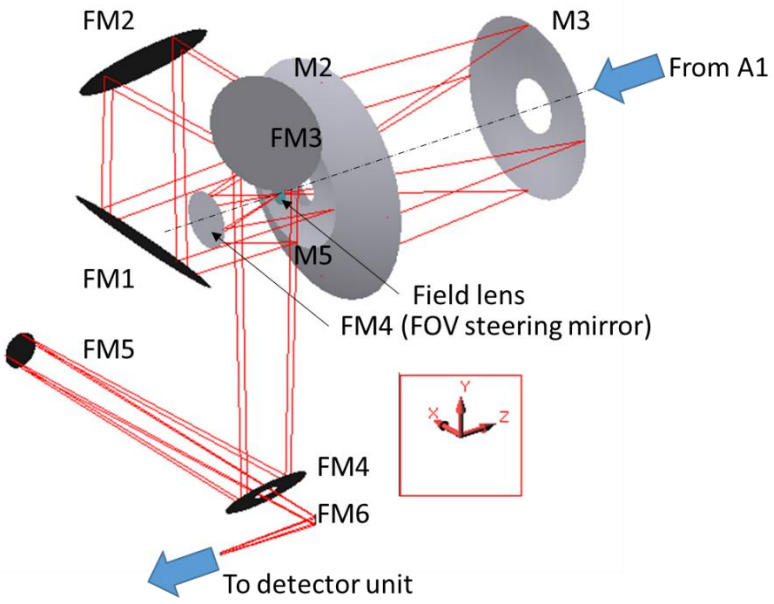

Fig. 6. Optical layout of OASIS corrector, scanner and folding optics. An intermediate image formed on a field lens by A1-M2-M3 optics. M4 (tip/tilt mirror) and M5 relays the intermediate image to single point where detector input port is placed. Folding optics FM1, 2, 3, 4 and 5 folds optical path.

2.4 Optics design procedure

Optical design procedure of inflatable primary antenna is summarized by the paper [7]. The process starts by parametrizing A1 antenna with base radius of curvature, and entrance pupil diameter. For Hencky surface, the diameter of A1 and baser radius of curvature R1 uniquely determines second and 4th order aspheric coefficients of the surface. For pre-cut and pre-formed gore, the shape of A1 is numerically calculated for given diameter of A1 and R1. The corrector optics placed at M2. M3 is placed at a position where geometrical blur is minimized. The hole size of M2 and M3 determines effective geometrical collection area, therefore, minimizing the size of the holes are critical. The location of M3 placed at the

minimum blur position satisfies the requirement. Also the intermediate image of A1-M2-M3 antenna has to be positioned at a locations close to M2 to minimize the M2 hole size. Once A1-M2-M3 is optimized at FOVs, 0 and edge of the field, as-built wave aberration is analyzed. The as-built wave aberration in RMS is incorporated into Strehl intensity ratio as an approximation of coupling efficiency of the antenna optics to detector, in the following section.

2.5 Optical throughput analysis

The primary telescope along with scanner optics supports large geometrical photon collection are $A_{geometrical}$ on the order of 100-200 m2 as design. However, effective photon collection area, $A_{effective}$ decreases due to optical aberrations, reflectivity and transmission of optics, alignment error, as well as pointing errors. $A_{effective}$ is modelled by,

$$A_{effective} = T_{optics} e^{-(2\pi\sigma)^2} A_{geometrical} \qquad (3)$$

,where T_{optics} is lumped sum of transmission of optics. Decomposition of the optical transmission T_{optics} is tabulated in Table 3. Loss of 0.5mil black Kapton is measured by ATR, and measurement result is shown in Fig. 7.

Table 3. Estimated loss of optical components

Element	Type	Size	Material	Loss
C1	Canopy	Ø19m	0.5mil black Kapton	0.24*
E1	Equatorial Web		Teflon (5% Areal filling factor)	0.02
A1	Pre-cut-gore reflector	Ø19m	Aluminized Film	0.01
M2	Asphere	Ø0.54m	Aluminized CFRP	0.01
M3	Asphere	Ø0.46m	Aluminized CFRP	0.01
Field Lens	Sphere	Ø0.05m	High Resistivity AR coated Si	0.05
M4	Flat	Ø0.26m	Aluminum	0.01
M5	Asphere	Ø0.3m	Aluminum	0.01
FM1	Flat, Elliptical	0.27x0.38m	Aluminum	0.01
FM2	Flat, Elliptical	0.24x0.34m	Aluminum	0.01
FM3	Flat, Elliptical	0.21x0.30m	Aluminum	0.01
FM4	Flat, Elliptical	0.15x0.22m	Aluminum	0.01
FM5	Flat, Segmented	Ø0.1m	Aluminum	0.01
FM6	Flat	Ø0.03	Aluminum	0.01
Total				0.38

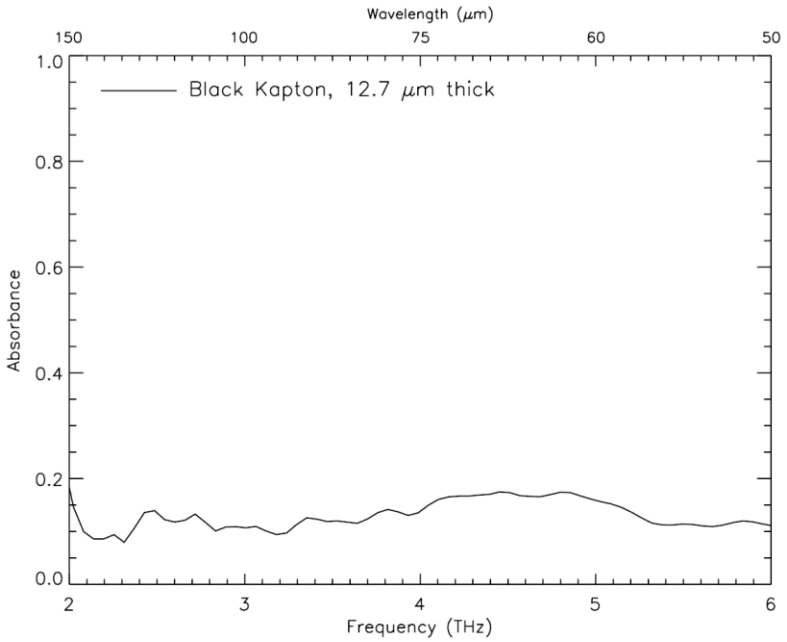

Fig. 7. Absorbance as a function of frequency in THz. Corresponding wavelength is indicated at the upper abscissa. Courtesy of Dr. Carrie Anderson at NASA Goddard Space Flight Center.

The team σ^2 is as built and FOV-averaged variance of the wave aberration that takes into account variation of wave aberration over the FOV. Detailed derivation of the $A_{effective}$ is described in the paper [7] and was calculated by wavefront error based tolerancing. Based on the values σ^2 effective photon collection area are estimated by parametrizing the design space with base radius of A1 and EPD as two primary variables. A detailed analysis is shown in the paper by Sid. Et al. [7]. Table 4 shows effective collection area. The design space analysis shows, the R1=50m, EPD = 17m design provides $A_{effective}$ 113 ~ 197.8 [m^2] without taking into account the optical loss, and manufacturing tolerances, tabulated in Table 5.

Table 4. Effective photon collection area

	Effective photon collection area [m^2]
Band 1 (658.88 to 521.38 μm)	197.8 m^2
Band 2 (272.54 to 136.27 μm)	189.74 m^2
Band 3 (121.13 to 104.28 μm)	148.21 m^2
Band 4 (81.42 to 81.2 μm)	113 m^2

Table 5. Wave aberration as-built performance summary

	Wave aberration in RMS [um]
A1-M2-M3, On-axis/Off-axis	4.28/7.65
Total system, On-axis/Off-axis	5.61/4.17

2.6 Active correction of thermal deformation of A1 mirror and space craft jitter

The OASIS observatory targets scientific objects by pointing space craft as well as internal FOV scanning mechanism depicted in Fig. 4. Upon pointing of targets by space craft, the temperature distribution over the A1 surface changes as Cosine -1/4 law [3]. Consequently, there is a deformation of A1 surface which is not axially symmetrical. Such effect is recently tested by a small scale system in thermal vacuum chamber [9]. The small scale system is a Hencky mirror with a 1m physical diameter. A region of 525mm diameter out of 1m mirror region was monitored as a function of temperature variation [9]. The effect of thermal deformation of A1 mirror is of great interest and now FEM analysis in on-going. The small scale 1m test indicates that some sorts of mitigation of such a non-symmetrical deformation is required. A 6 segmented mirror (FM5 in Fig. 6) is placed to correct for the A1 deformation. Each of the mirror has a 3 DOF (tip, tilt and piston) which is controlled by Stochastic Parallel Gradient Decent (SPGD) algorithm. First, one of the segmented mirror is actuated while observing signal from Band 4 detector. The process is repeated for the rest of the segmented mirrors by determining the sign and range of actuation of the 3 DOFs.

3. CONCLUSIONS

Optical design of all reflective, except for a thin field lens element, THz telescope design with a 17m class inflatable primary antenna for Orbiting Astronomical Satellite for Investigating Stellar Systems (OASIS) mission involves well-defined functionality of each subcomponents. The inflatable primary A1 and corrector optics M2 and M3 forms an intermediate image which is relayed to detector by scanning optics. The optimum optical arrangement is identified that maximizes geometrical photon collection area while minimizing size and weight of corrector optics for spherical aberration by A1. The shape of A1, for example Hencky or pre-formed and pre-curt gore based quasi parabola impacts on overall system size primarily via size of M2 and M3 corrector. Current 17m inflatable antenna design achieves over 113 m of photon collection area while limiting the corrector optics size of about 0.6m in diameter.

REFERENCES

[1] Walker C. K., Chin G., Arenberg J. W., Kim D., Takashima Y., “Orbiting Astronomical Satellite for Investigating Stellar Systems (OASIS) Following the Water Trail from the Interstellar Medium to Oceans,” Accepted for SPIE Optics and Photonics, Astronomical Optics: Design, Manufacture, and Test of Space and Ground Systems III (2021).

[2] Arenberg J. W., Pohner J., Harpole G., Walker-Horne A., Nolan M., McGregor D., Moore K, Takashima Y., Veal G., Palisoc A., Kim D, Walker C. K., “Design and performance of the Orbiting Astronomical Satellite for Investigating Stellar Systems (OASIS)” Accepted for SPIE Optics and Photonics, Astronomical Optics: Design, Manufacture, and Test of Space and Ground Systems III (2021).

[3] Arenberg J. W., Villarreal M. N., Harpole G., McGregor R. D., Walker-Horn A., Pohner J., Moore K., Clithero A.,, Harris L., Meyer T., and A. L. Palisoc, “Environmental Challenges to OASIS’s Primary Reflector”, Accepted for SPIE Optics and Photonics, Astronomical Optics: Design, Manufacture, and Test of Space and Ground Systems III (2021).

[4] Hencky, H., “Über den Spannungszustand in kreisrunden Platten,” Zeitschrift für Angew. Math. und Mech., 311–317 (1915).

[5] Palisoc A. L. Pardoen G., Takashima Y., Chandra A., Sirshi S., Choi H., Kim D., Quach H., Arenberg J. W. and Walker C., “Analytical and finite element analysis tool for nonlinear membrane antenna modeling for astronomical applications”, Accepted for SPIE Optics and Photonics, Astronomical Optics: Design, Manufacture, and Test of Space and Ground Systems III (2021).

[6] Offner A., "A Null Corrector for Paraboloidal Mirrors," Appl. Opt. 2, 153-155 (1963)

[7] Siddhartha, S., Takashima Y ., Palisoc A., Chandra A.,., Walker C. K., Kim D.. " Parametric design study of the Orbiting Astronomical Satellite for Investigating Stellar Systems (OASIS) space telescope ," Accepted for SPIE Optics and Photonics, Astronomical Optics: Design, Manufacture, and Test of Space and Ground Systems III (2021).

[8] Walker, Christopher K. Terahertz Astronomy. Baton Rouge: CRC, 2016. Web.

[9] Quach H., Esparza M., Kang H., Chandra A., Choi H., Berkson J., Karrfalt K., Sirsi S., Takashima Y., Palisoc A., Arenberg J. W. Gogick Marshall K., Glynn C. S., Godinez S. M., Tafoya M., Walker C., d’Aubigny C. D., and Kim D., “Deflectometry-Based Thermal Vacuum Testing for a Pneumatic Terahertz Antenna”, Accepted for SPIE Optics and Photonics, Astronomical Optics: Design, Manufacture, and Test of Space and Ground Systems III (2021).